

Electronic structure, magnetic and optical properties of intermetallic compounds R_2Fe_{17} ($R = Pr, Gd$)

Yu.V. Knyazev,¹ A.V. Lukoyanov,^{1,2} Yu.I. Kuz'min,¹ A.G. Kuchin,¹ and I.A. Nekrasov^{1,3}

¹Institute of Metal Physics, Russian Academy of Sciences-Ural Division,
620041 Yekaterinburg GSP-170, Russia

²Ural State Technical University-UPI, 620002 Yekaterinburg, Russia

³Institute of Electrophysics, Russian Academy of
Sciences-Ural Division, 620046 Yekaterinburg, Russia

(Dated: February 7, 2022)

Abstract

In this paper we report comprehensive experimental and theoretical investigation of magnetic and electronic properties of the intermetallic compounds Pr_2Fe_{17} and Gd_2Fe_{17} . For the first time electronic structure of these two systems was probed by optical measurements in the spectral range of 0.22–15 μm . On top of that charge carriers parameters (plasma frequency and relaxation frequency) and optical conductivity (!) were determined. Self-consistent spin-resolved bandstructure calculations within the conventional LSDA + U method were performed. Theoretical interpretation of the experimental (!) dispersions indicates transitions between 3d and 4p states of Fe ions to be the biggest ones. Qualitatively the line shape of the theoretical optical conductivity coincides well with our experimental data. Calculated by LSDA + U method magnetic moments per formula unit are found to be in good agreement with observed experimental values of saturation magnetization.

PACS numbers: 71.20.-b, 78.20.-e, 75.50.Ww

I. INTRODUCTION

During last two decades Fe-rich intermetallic systems stay under investigation from both experimental and theoretical points of view because of its anomalous magnetic properties. At present the intermetallic compounds with rare-earth elements draw a significant interest because of their well pronounced Invar properties and also as possible new cheap high-energy storing materials for permanent magnets.^{1,2,3,4,5,6,7} Rare-earth intermetallic compounds R_2Fe_{17} (R = a rare-earth ion) are well-known due to large magnetic moment of Fe ions and yet their comparatively low Curie temperature T_C . Further increase of the T_C of the compounds can be achieved by implantation of interstitial atoms^{1,2} or introducing a low content of non-magnetic impurities substituting Fe atoms.^{3,4,5,6,7} In such extended systems, compared to the parent R_2Fe_{17} compounds, upon the doping T_C grows more than twice in some cases. This increment of T_C was explained primarily as a result of the lattice expansion with substitution of Fe ions for larger radii ions. According to this concept, Fe-Fe interactions are ferromagnetic or antiferromagnetic for interatomic distance larger or smaller than the critical value 0.25 nm.⁸ However, a number of experiments^{9,10,11} showed that in the substitutional $R_2Fe_{17-x}Si_x$ alloys the crystal lattice contracts and the magnetic moment per unit volume decreases, while T_C grows. Later experimental facts are in apparent contradiction with the model.⁸ Clearly, a simple approach based on distance-dependent exchange interaction is not sufficient to explain the changes of magnetic properties of these compounds with substitution of Fe for non-magnetic ions.

Past few years several results of band structure calculations of the systems from the family are available. For instance the spin-polarized calculations of electron spectra of $Y_2Fe_{17}N_3$,¹² $Sm_2Fe_{17-x}M_x$ ($M = Al, Ga, Si$),¹³ and $Nd_2Fe_{17-x}M_x$ ($M = Si, Ga$)¹⁴ compounds showed that non-magnetic impurities modify the shape and width of the spin-up and spin-down densities of states $N(E)$. Jaswal et al.¹² suggested to explain the increase of T_C in $Y_2Fe_{17}N_3$ via changes of the density of states at the Fermi level $N(E_F)$ owing to the lattice expansion by means of the Mohn-Wohlfarth static spin-fluctuation model.¹⁵ An analysis of the experimental optical,^{7,16,17} low-temperature heat capacity⁷ and photoemission¹⁸ data of some pseudobinary alloys $R_2Fe_{17-x}M_x$ with $M = Al, Si$ revealed a qualitative correlation between the Curie temperature and parameters of electronic structure in frame of such an approach. Recent experimentally measured optical conductivity of Ce_2Fe_{17} was interpreted in terms of

band structure obtained within local density approximation (LDA).¹⁹

In accordance with the foregoing systematic study of the electronic structure of R_2Fe_{17} compounds and their modifications with substituted Fe ions further investigations are of fundamental importance. In this work theoretical calculations of the electronic properties together with experimental magnetic and optical measurements were performed. The paper is organized as follows: in the section II experimental details and results for Pr_2Fe_{17} and Gd_2Fe_{17} are presented. For instance, subsection IIA is devoted to sample preparation, X-ray diffraction structural analysis and magnetic measurements conditions. Subsection IIB provides description of optical experiments. Section III contains results of LSDA + U²⁰ computations of electronic structure and magnetic properties of R -Fe and Gd -Fe systems. Structure of experimentally observed optical conductivity curves is analyzed in the section IV. At the end we briefly summarize our paper with the section V.

II. EXPERIMENT

A. Samples and magnetic measurements

The compounds Pr_2Fe_{17} and Gd_2Fe_{17} were prepared by induction melting in alumina crucible under argon atmosphere. The ingots were homogenized in the high-purity argon atmosphere at 1300 K. The purity of the alloys was checked using standard X-ray diffraction in $Cu K\alpha$ radiation. The samples were found to be polycrystalline, single-phase and have rhombohedral structure of the Th_2Zn_{17} -type²¹ (space group $R\bar{3}m$) for Pr_2Fe_{17} and hexagonal crystal structure of the Th_2Ni_{17} -type²² (space group $P6_3/mmc$) for Gd_2Fe_{17} . The measured lattice parameters a and c are close to those published earlier^{21,22} and are shown in the Table I. Spherical specimens of 2–3 mm in diameter were used for magnetic measurements. For following optical studies the specular surface of the samples was prepared by mechanical polishing with diamond pastes.

The Curie points of the compounds were determined from temperature dependencies of ac susceptibility. The ac susceptibility was measured by a differential method in an ac magnetic field of 8 Oe with a frequency of 80 Hz. The saturation magnetizations at $T = 4.2$ K were determined from the isothermal magnetization measurements carried out by means of vibrating sample magnetometer in magnetic fields up to 20 kOe. The magnetic parameters

TABLE I: Experimental structural, magnetic, and electronic parameters of the intermetallic compounds $\text{Pr}_2\text{Fe}_{17}$ and $\text{Gd}_2\text{Fe}_{17}$: lattice parameters a , c ; unit-cell volume at room temperature V ; T_C { Curie temperature; M_s { spontaneous magnetization at $T = 4.2$ K; relaxation and plasma frequencies; N_{eff} { effective concentration of conduction electrons.

Compound	a (Å)	c (Å)	V (Å ³)	T_C (K)	M_s (B/f.u.)	$(10^{13} \text{ s}^{-1})^2$	(10^{30} s^{-2})	N_{eff} (10^{22} cm^{-3})
$\text{Pr}_2\text{Fe}_{17}$	8.579	12.472	795.0	294	36.1	1.9	21.3	0.67
$\text{Gd}_2\text{Fe}_{17}$	8.496	8.341	521.4	466	21.2	1.5	19.5	0.61

of the compounds are listed in Table I. They are a little different from previously reported data.^{23,24} The differences among authors may originate from some deviations of their samples from stoichiometry.

B. Optical measurements

Investigation of optical properties of $\text{Pr}_2\text{Fe}_{17}$ and $\text{Gd}_2\text{Fe}_{17}$ were carried out at room temperature by ellipsometric Beattie technique.²⁵ Spectroscopic ellipsometry is based on the fact that the state of polarization of incident light is changed on reflection. The optical constants { refractive index n and absorption coefficient k } were measured in the spectral range of $\hbar\omega = 0.077\{5.6 \text{ eV}$ (ω is a cyclic frequency of light) with accuracy of 2{4%. From n and k , the real $\epsilon_1(\omega) = n^2 - k^2$ and imaginary $\epsilon_2(\omega) = 2nk$ parts of the complex dielectric function $\epsilon(\omega)$, the optical conductivity $\sigma(\omega) = nk\omega/2$, and the reflectance $R(\omega) = [(n - 1)^2 + k^2] / [(n + 1)^2 + k^2]$ were derived. Measurements of reflection spectra followed by the Kramers-Kronig analysis were applied to determine the optical parameters in the short-wave range ($\hbar\omega = 5.6\{8.5 \text{ eV}$).

The results of optical study ($n; k; \epsilon_1; \epsilon_2; R$ as functions of ω) for the Pr and Gd compounds are shown in Fig. 1. It is seen that the optical properties of both compounds are rather similar. All directly measured dispersions and further derived quantities are characterized by the broad feature with maximum at the photon energies near 1 eV. As it follows from the lineshape of the $\epsilon_2(\omega)$, there is a strong absorption region at energies $\hbar\omega > 1 \text{ eV}$. With increase of the wavelength to infrared range ($\lambda > 2 \text{ }\mu\text{m}$) (inset of Fig. 1a) the nonmonotonic behaviour of n and k is changed by a smooth growth related to the domination of free-electron

absorption. Such a character of the frequency dependencies for the optical constants together with negative quantities ϵ_1 , as a rule, is typical for the metal-like solids. As one can see from dispersion curves $R(\omega)$, in the low-energy range the reflectance exhibits the high values. The analysis of the energy dependence of ϵ_1 and ϵ_2 in this spectral interval, corresponding to intraband electronic excitations, makes it possible to determine the plasma frequency and the effective relaxation frequency of free charge carriers. Within the assumption that light absorption for these energies has Drude character, the parameters $\omega_p^2 = \omega_1^2(\epsilon_1^2 + \epsilon_2^2) = \epsilon_1$ and $\omega_r^2 = \epsilon_2/\epsilon_1$ were computed. In the long-wave region $\lambda > 8 \text{ } \mu\text{m}$, ω_p^2 and ω_r^2 become frequency independent. The values of ω_p and ω_r in this energy interval were used then to estimate the effective concentration of conduction electrons $N_{\text{eff}} = \omega_p^2 m / 4 e^2$ (m and e are the mass and the charge of a free electron respectively). All these parameters obtained from experimental data treatment are presented in Table I.

Optical conductivities $\sigma(\omega)$ for both compounds are displayed in Fig. 2. A monotonic increment of the experimental $\sigma(\omega)$ dispersion observed in the low-energy range is related to the Drude mechanism of electron excitations. For both systems intraband (Drude-like) contribution to the optical conductivity were computed according to the relation $\sigma_{\text{Intra}}(\omega) = \omega_p^2 / 4(\omega_1^2 + \omega^2)$ and drawn in Fig. 2 black dotted lines. Corresponding values of ω_p^2 and ω_r^2 are given in Table I. The magnitude of these contributions falls down sharply with energy and becomes insignificant above 0.5 eV. The values of static conductivity $\sigma_{\text{Intra}}(0)$ are estimated to be $0.89 \cdot 10^{16} \text{ s}^{-1}$ for $\text{Pr}_2\text{Fe}_{17}$ and $1.03 \cdot 10^{16} \text{ s}^{-1}$ for $\text{Gd}_2\text{Fe}_{17}$ correspondingly. With increase of photon energy the $\sigma(\omega)$ curves show a very intense asymmetric structures in the near infrared region of spectra at 1.2 eV. These structures have a pronounced shoulder on high-energy side and abrupt low-energy edge. Such a behaviour is a typical manifestation of the predominance of the interband absorption in this energy interval. The similar shape of the $\sigma(\omega)$ curves was early observed in Y_2Fe_{17} , $\text{Ce}_2\text{Fe}_{17}$, and $\text{Lu}_2\text{Fe}_{17}$ compounds.¹⁷

III. ELECTRONIC STRUCTURE CALCULATIONS

To calculate electronic structure of the intermetallic compounds under investigation LSDA+U method²⁰ within the TB-LMTO-ASA package (Tight Binding, Linear Muffin-Tin Orbitals, Atomic Sphere Approximation)²⁶ was applied. Experimentally obtained values of lattice constants for both Pr and Gd systems given in Table I were used in our calcula-

tions. Atomic spheres radii were chosen as $R(\text{Pr}) = 3.91 \text{ a.u.}$ and $R(\text{Fe}) = 2.62 \text{ a.u.}$ for $\text{Pr}_2\text{Fe}_{17}$ and $R(\text{Gd}) = 3.72 \text{ a.u.}$ and $R(\text{Fe}) = 2.66 \text{ a.u.}$ for $\text{Gd}_2\text{Fe}_{17}$. Orbital basis consists of 6s, 6p, 5d, and 4f mu n-tin orbitals for Pr or Gd and 4s, 4p, and 3d for Fe sites. The calculations were performed with 32 irreducible k-points ($6 \times 6 \times 6$ spacing) in the 1st Brillouin zone. Parameters of direct U and exchange J Coulomb interactions for Gd and Pr ions were calculated by constrained LDA method.²⁷ For $\text{Gd}_2\text{Fe}_{17}$ we obtained $U_{\text{Gd}} = 6.7 \text{ eV}$ and $J_{\text{Gd}} = 0.7 \text{ eV}$ (similar values were determined previously for elemental Gd²⁰), and for $\text{Pr}_2\text{Fe}_{17}$ $U_{\text{Pr}} = 4.9 \text{ eV}$ and $J_{\text{Pr}} = 0.6 \text{ eV}$. Corresponding values of U and J were applied to Gd and Pr compounds in frame of the LSDA+ U method. To note, in the present work we do not take into account local Coulomb interaction on Fe ions since constrained LDA gives surprisingly large U values.²⁸ However, for elemental Fe it was shown that account of Coulomb correlations is important to describe semiquantitatively temperature dependence of magnetization.²⁹ But on the other hand such approach reproduces main structures of LSDA DOS with slight modifications of the Fe 3d DOS and thus in our case will not affect resulting dispersions of optical conductivity strongly.

Total magnetic moments per formula units obtained within LSDA+ U method ($33.79 \mu_B$ for $\text{Pr}_2\text{Fe}_{17}$ and $21.89 \mu_B$ for $\text{Gd}_2\text{Fe}_{17}$) are in good agreement with measured experimental data (see Table I). Values of local magnetic moments for different sites for $\text{Pr}_2\text{Fe}_{17}$ and $\text{Gd}_2\text{Fe}_{17}$ compounds are listed in Table II. Pr and Gd 4f-shells are computed to be fully polarised with local moments close to its ionic values while Fe ions have local moments values almost equal to its elemental Fe magnitude. It is remarkable that local moments on rare-earth sites during selfconsistent loops become oppositely directed to those on Fe sites. One should also mention that initial value of local moments on Pr and Gd ions was taken to be zero. Thus R and Fe sublattices in our calculations are obtained to be antiferromagnetically ordered.

Calculated in the present work within the LSDA+ U method partial Fe 4p;3d and rare-earth 5d;4f DOS for spin-up (") and spin-down (#) projections of local spin moments for $\text{Pr}_2\text{Fe}_{17}$ and $\text{Gd}_2\text{Fe}_{17}$ are shown in Figs. 3 and 4. It is seen that main spectral weight is located in the $E_F - 5 \text{ eV}$ energy range around the Fermi level. Structures of these DOS are rather similar for both compounds and are qualitatively close to the DOS of ferromagnetic elemental iron in bcc structure.³⁰ Both these spin-polarized DOSs have a two-peak structure related to the 3d states of Fe ions. The Fermi level E_F set to zero lies near the minimum

TABLE II: Calculated within the LSDA + U method values of local magnetic moments for different sites in $\text{Pr}_2\text{Fe}_{17}$ and $\text{Gd}_2\text{Fe}_{17}$ compounds.

$\text{Pr}_2\text{Fe}_{17}$		$\text{Gd}_2\text{Fe}_{17}$	
Site	M (μ_B)	Site	M (μ_B)
Pr(6c)	2.08	Gd(2b)	7.13
Fe(6c)	2.21	Gd(2d)	7.20
Fe(9d)	2.23	Fe(4f)	2.31
Fe(18f)	2.13	Fe(6g)	2.10
Fe(18h)	2.34	Fe(12j)	2.40
		Fe(12k)	1.87

between these two peaks in the spin-down channel and on the upper edge in the spin-up channel. "Spin-up" states of Fe ions are almost completely occupied while "spin-down" are nearly half-filled. The narrow intensive peaks at 3 eV (#) and 2.7 eV (") ($\text{Pr}_2\text{Fe}_{17}$) also at 7.3 eV (#) and 3.5 eV (") ($\text{Gd}_2\text{Fe}_{17}$) belong to 4f states of rare-earth ions. The intensities of Fe 4s;4p and rare-earth 6s;6p, and 5d contributions to the DOS are considerably smaller.

IV. ANALYSIS OF OPTICAL CONDUCTIVITY STRUCTURE

Calculated LSDA + U band structures presented in the preceding section were used to interpret experimental optical conductivity (!) for both intermetallic systems under consideration. In order to calculate theoretical optical conductivity $\sigma_{\text{theor}}(!)$ and analyze its ingredients we applied rather simplified technique similar in spirit to Ref.³¹. Namely, we computed following convolutions representing all possible optical transitions

$$\sigma_{\text{is}}^0(!) = \frac{1}{\pi} \int_{E_F}^{E_F + \hbar\omega} N_{i1}^s(E) N_{i1^0}^s(E - \hbar\omega) dE; \quad (1)$$

where $N_{i1}^s(E)$ and $N_{i1^0}^s(E)$ are partial DOSs of the same ion i with the same spins and orbital quantum numbers l and l^0 shown in Figs. 3 and 4. The orbital quantum numbers are related by dipole selection rule $l - l^0 = \pm 1$. Total theoretical optical conductivity is linear combination of different contributions (1):

$$\sigma_{\text{theor}}(!) = \sum_{i,l,l^0=\pm 1} m_i \sigma_{\text{is}}^{l,l^0}(!); \quad (2)$$

where m_i is the degrees of site degeneracy (Wycko positions).

Figs. 2 and 5 display corresponding $\epsilon_{\text{theor}}(\omega)$ as solid lines. The overall shape of optical conductivity dispersion curves for both compounds exhibits a broad structure with the peak at ~ 2 eV. On the whole the theoretical calculations reproduce main features of the experimental $\epsilon(\omega)$ curve (Fig. 2): (i) the width of the intense absorption band with distinct maximum, (ii) the sharp threshold in the 0.5–1 eV range and (iii) the gradual diminution of the high-energy slope.

At the same time there are certain discrepancies. The theoretical peaks are slightly shifted towards the higher energies in contrast to the experimental ones. Also high-energy contributions at 4 eV are slightly overestimated. It may have following reasons. As was shown by Lichtenstein et al.²⁹ inclusion of local dynamical Coulomb interactions into consideration in elemental Fe will lead to about 30% of correlation bandwidth narrowing. In our case DOS in the vicinity of the Fermi level consists mostly from Fe 3d states which are almost identical to those of elemental bcc iron. Roughly one can say that for our intermetallic compounds it can slightly improve comparison with experiment. First of all peak at 2 eV could be moved on 0.5–0.6 eV towards lower energies because of correlation narrowing. Second spectral weight at 4 eV can be transferred to lower energies and it can give high-energy tail of theoretical optical conductivity closer to experimental one. Furthermore for both systems $\epsilon_{\text{theor}}(\omega)$ shows a significant interband absorption in the low-energy range ($\sim \omega < 0.6$ eV) which was not confirmed by the measurements. It is possible that the low-energy absorption, predicted in theory, may be partially disguised in the experimental $\epsilon(\omega)$ curves by the strong Drude rising. The Drude contribution was not taken into consideration in our theoretical model.

Densities of states near the Fermi energy for both compounds mostly consist of the 3d-states of various crystallographically inequivalent iron ions (see Figs. 3 and 4). A line shape of our LSDA calculated Fe ions DOS is very similar to the known DOS of elemental Fe in the bcc (hcp) phase.^{30,32} For the bcc iron it was shown³³ that the optical conductivity determined using the Berglung-Spicer approach³¹ agrees rather well with theoretical calculations accounting matrix elements³⁴ and also with experimental results.³⁵ This fact enables us to suppose that matrix elements formalism does not play an important role in case of intermetallic compounds $R_2\text{Fe}_{17}$. In this work we can report our theoretical curves to be in a reasonable qualitative agreement with experimental data.

To analyze the line shape of experimental $\epsilon(\omega)$ we provide detailed description of different

contributions to $\sigma_{\text{theor}}(\omega)$. As it is seen in Fig. 5 for both systems biggest contribution to $\sigma_{\text{theor}}(\omega)$ comes from 3d{4p interband optical transitions for Fe ions through the spin-down channel. That gives a high absorption peak at ~ 2 eV (see dotted curves in Fig. 5). These particular transitions mostly govern low-energy range behaviour below 1 eV as well. Second largest contribution is 3d{4p transitions for Fe ions but in the spin-up channel. In Fig. 5 one can see it as a rather broad structure with maxima at ~ 4 eV (dot-dashed curves). The contributions from Fe 4s-4p (Fig. 5, dashed-dot-dot lines) and Pr(Gd) 4f-5d (Fig. 5, thin solid line) transitions are substantially smaller; and magnitude of convolutions of rare earths 5d-6p and 6s-6p states is negligible.

V. SUMMARY

Comprehensive experimental investigation of structural, magnetic and optical properties of the intermetallic compounds $\text{Pr}_2\text{Fe}_{17}$ and $\text{Gd}_2\text{Fe}_{17}$ was performed during this work. Refined structural parameters are found to be in good agreement with previous data. Measured magnetic properties: (i) Curie temperatures $T_C = 294\text{K}$ (466K) and (ii) saturation magnetizations (at $T = 4.2\text{K}$) 36.1 (21.2) $\mu_B/\text{f.u.}$ for Pr-Fe (Gd-Fe) systems respectively also agree well with available in the literature experimental data. We also report measured for the first time optical constants n and k observed at room temperature by ellipsometric Beattie technique in the spectral range of $0.22\{15$ μm . This experimental data allows us to determine charge carriers parameters (plasma and relaxation frequencies) and optical conductivity $\sigma(\omega)$.

To model magnetic and optical properties of $\text{Pr}_2\text{Fe}_{17}$ and $\text{Gd}_2\text{Fe}_{17}$ we did self-consistent spin-resolved calculations within the LSDA+U method. Calculated by LSDA+U method magnetic moments per formula unit describe well observed experimental values. Furthermore experimental optical conductivity $\sigma(\omega)$ was interpreted in terms of convolutions between partial densities of states for the same ion applying dipole selection rule for orbital quantum number. Overall the line shape of experimental and theoretical optical conductivity curves was found to be qualitatively very similar. By analyzing different contributions to $\sigma_{\text{theor}}(\omega)$ it was understood that transitions between 3d and 4p states of Fe ions give the biggest contribution. The intense peaks in optical conductivity below 1 eV and around 2 eV are predominantly formed by the transitions in the "spin-down" channel while the second

large contribution from "spin-up" channel transitions provides broad feature with the maximum at about 4 eV. The other contributions from rare-earth 4f-5d and iron 4s-4p optical transitions are almost negligible.

VI. ACKNOWLEDGMENTS

This work was supported by Grants of Russian Foundation for Basic Research 05-02-17244, 04-02-16086 and 05-02-16301 and in part by programs of the Presidium of the Russian Academy of Sciences (RAS) "Quantum macrophysics" and of the Division of Physical Sciences of the RAS "Strongly correlated electrons in semiconductors, metals, superconductors and magnetic materials". Two of us (IN, AL) acknowledge Dynasty Foundation and International Center for Fundamental Physics in Moscow and Russian Science Support Foundation (IN).

-
- ¹ J. M. D. Coey and H. Sun, *J. Magn. Magn. Mater.* **87**, L251 (1990); H. Sun, J. M. D. Coey, Y. Otani, and D. P. F. Hurley, *J. Phys.: Condens. Matter* **2**, 6465 (1990).
 - ² D. B. de Mooij, K. H. J. Buschow, *J. Less-Common Met.* **142**, 349 (1988).
 - ³ P. C. M. Gubbens, A. M. Van Der Kraan, T. H. Jacobs, and K. H. J. Buschow, *J. Less-Common Met.* **159**, 173 (1990).
 - ⁴ T. H. Jacobs, K. H. J. Buschow, G. F. Zhou, X. Li, and F. R. de Boer, *J. Magn. Magn. Mater.* **116**, 220 (1992).
 - ⁵ Z. Wang and R. A. Dunlap, *J. Phys.: Condens. Matter* **5**, 2407 (1993).
 - ⁶ B. G. Shen, F. W. Wang, L. S. Kong, and L. Cao, *J. Phys.: Condens. Matter* **5**, L685 (1993).
 - ⁷ A. G. Kuchin et al., *Phys. Stat. Sol. (a)* **155**, 479 (1996).
 - ⁸ D. Givord, R. Lemaire, *IEEE Trans. Magn. MAG-10*, 109 (1974).
 - ⁹ R. van Mens, *J. Magn. Magn. Mater.* **61**, 24, (1986).
 - ¹⁰ Z. W. Li, X. Z. Zhou, and A. H. Morrish, *Phys. Rev. B* **51**, 2891 (1995).
 - ¹¹ A. G. Kuchin, A. S. Ermolenko, V. I. Khrabrov, *Phys. Met. Metallogr.* **86**, 276 (1998).
 - ¹² S. S. Jaswal, W. B. Yelon, G. C. Hadjipanayis, Y. Z. Wang, and D. J. Sellmyer, *Phys. Rev. Lett.* **67**, 644 (1991).

- ¹³ R. F. Sabirianov and S. S. Jaswal, *J. Appl. Phys.* 79, 5942 (1996).
- ¹⁴ Ming-Zhu Huang and W. Y. Ching, *J. Appl. Phys.* 79, 5545 (1996).
- ¹⁵ P. Mohn and E. P. Wohlfarth, *J. Phys. F: Met. Phys.* 17, 2421 (1987).
- ¹⁶ Yu. V. Knyazev, A. G. Kuchin, and Yu. I. Kuz'min, *Phys. Met. Metallogr.* 89, 558 (2000).
- ¹⁷ Yu. V. Knyazev, A. G. Kuchin, and Yu. I. Kuz'min, *J. Alloys Comp.* 327, 34 (2001).
- ¹⁸ J. P. Woods et al., *Phys. Rev. B* 51, 1064 (1995).
- ¹⁹ I. A. Nekrasov, Yu. V. Knyazev, Yu. I. Kuz'min, A. G. Kuchin, and V. I. Anisimov, *Phys. Met. Metallogr.* 97 (2), 129 (2004).
- ²⁰ V. I. Anisimov, F. Aryasetiawan, and A. I. Lichtenstein, *J. Phys.: Condens. Matter* 9, 767 (1997).
- ²¹ Q. Johnson, D. H. Wood, and G. S. Smith, *Acta Crystallographica B* 24, 274 (1968).
- ²² F. Givord and R. Lemaire, *J. Less-Common Met.* 21, 463 (1970).
- ²³ X. C. Kou, F. R. de Boer, R. Grossinger, G. Wiesinger, H. Suzuki, H. Kitazawa, T. Takamasu, G. Kido, *J. Magn. Mater.* 177-181, 1002 (1998).
- ²⁴ R. C. Mohanty, C. Zhang, S. A. Shaheen, A. Murugiah, A. Raman, C. G. Grenier, and R. E. Ferrel Jr., *J. Phys.: Condens. Matter* 12, 9657 (2000).
- ²⁵ J. R. Beattie and G. M. Conn, *Philos. Mag.* 46, 235 (1955).
- ²⁶ O. K. Andersen, *Phys. Rev. B* 12, 3060 (1975).
- ²⁷ O. Gunnarsson, O. K. Andersen, O. Jepsen, and J. Zaanen, *Phys. Rev. B* 39, 1708 (1989).
- ²⁸ V. I. Anisimov and O. Gunnarsson, *Phys. Rev. B* 43, 7570 (1991).
- ²⁹ A. I. Lichtenstein, M. I. Katsnelson, and G. Kotliar, *Phys. Rev. Lett.* 87, 067205 (2001).
- ³⁰ O. Gunnarsson, *Physica BC* 91, 329 (1977).
- ³¹ C. N. Berglund and W. E. Spicer, *Phys. Rev.* 136, A1030 (1964); C. N. Berglund and W. E. Spicer, *Phys. Rev.* 136, A1044 (1964).
- ³² S. Wakon, J. Yamashita, *J. Phys. Soc. Japan* 21, 1712 (1966).
- ³³ G. A. Bolotin, M. M. Kirillova, V. M. Mavskii, *Phys. Met. Metallogr.* 27 (2), 224 (1969).
- ³⁴ M. Singh, C. S. Wang, and J. Callaway, *Physical Review B* 11, 287 (1975); K. J. Kim, T. C. Leung, B. N. Harmon, and D. W. Lynch, *J. Phys.: Condens. Matter* 6, 5069 (1994).
- ³⁵ V. P. Shirokovskii, M. M. Kirillova, N. A. Shilkova, *JETP* 82 (3), 784 (1982).

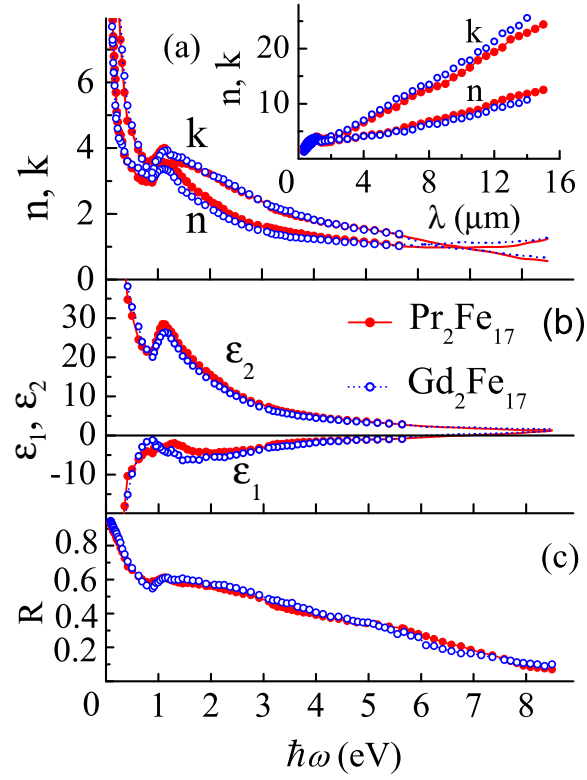


FIG. 1: (Color online) Experimental optical constants n and k (panel a), dielectric functions ϵ_1 and ϵ_2 (panel b), and reflectivity spectra R (panel c) for $\text{Pr}_2\text{Fe}_{17}$ (full circles and solid line) and $\text{Gd}_2\text{Fe}_{17}$ (empty circles and dotted line) compounds. Dotted and solid lines above 5.6 eV represent values obtained by Kramers-Kronig transformation from reflection spectra. Inset presents dependences of the optical constants on wavelength for an expanded view in infrared region.

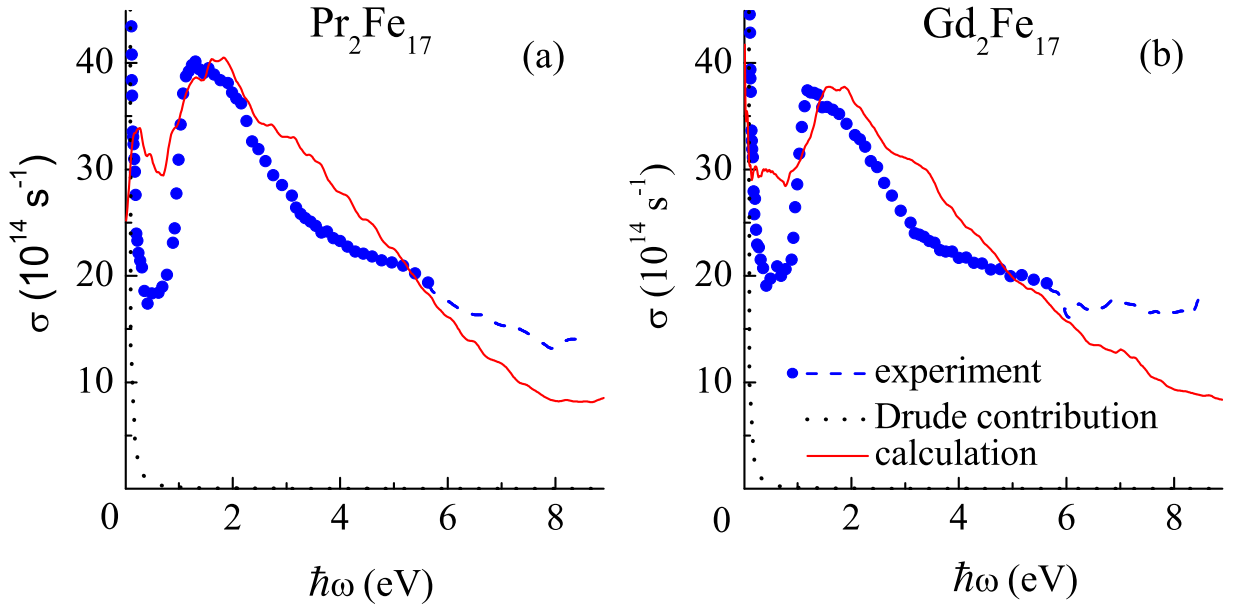


FIG. 2: (Colour online) Experimental (dark circles and dashed lines) and calculated (solid lines) dispersion dependencies of optical conductivity for $\text{Pr}_2\text{Fe}_{17}$ (a) and $\text{Gd}_2\text{Fe}_{17}$ (b) compounds. Dashed lines represent (!) values obtained by Kramers-Kronig transformation from reflection spectra. Dotted lines correspond to intraband contributions estimated by Drude formula. Calculated values are in arbitrary units.

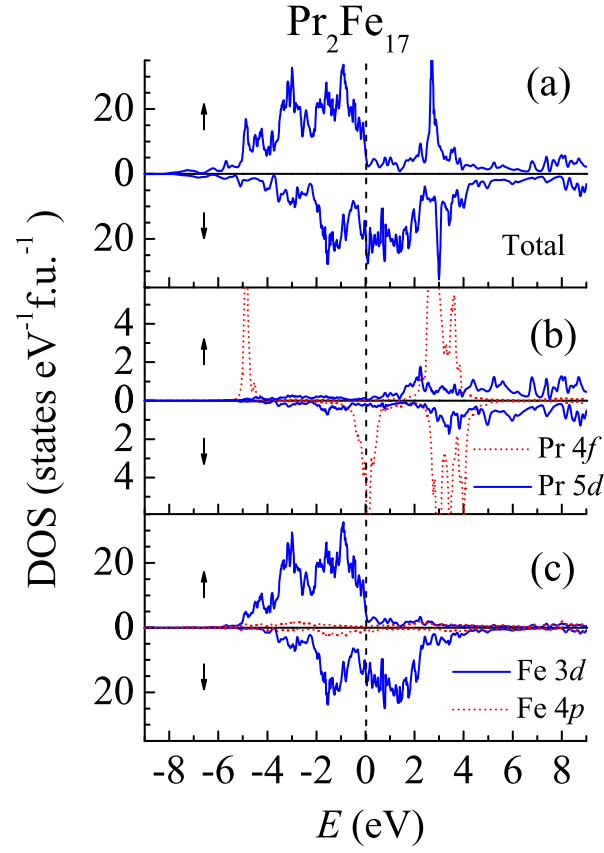


FIG. 3: (Colour online) Spin-resolved total (a) and partial 5d and 4f DOS of rare earth ion (Pr) (b) and 3d and 4p densities of states of Fe (c) for $\text{Pr}_2\text{Fe}_{17}$ compound obtained from the LSDA+U calculation. DOSs were smoothed using adjacent averaging in the interval 0.1 eV. The Fermi level corresponds to zero.

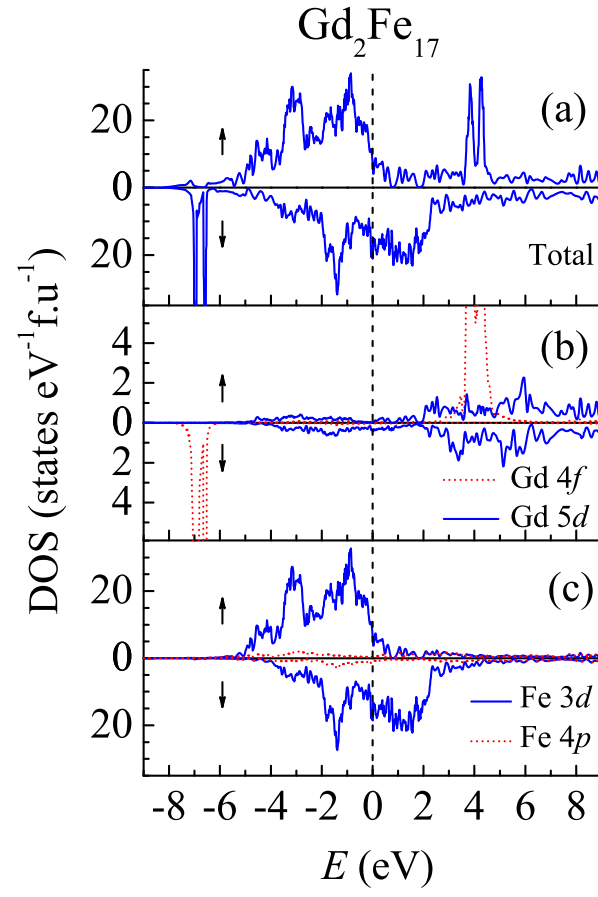


FIG. 4: (Colour online) The same as Fig. 3 but for $\text{Gd}_2\text{Fe}_{17}$.

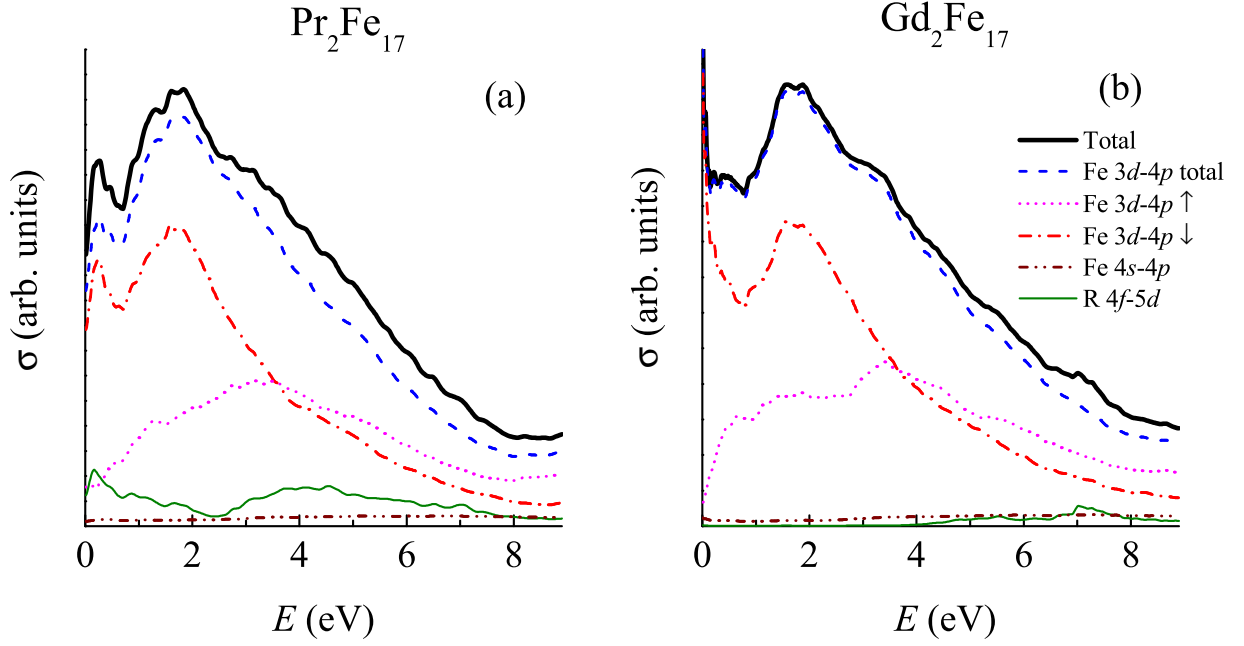


FIG .5: (Colour online) Calculated total (thick solid lines) and partial contributions in optical conductivity for $\text{Pr}_2\text{Fe}_{17}$ (a) and $\text{Gd}_2\text{Fe}_{17}$ (b) compounds. Dashed, dotted, and dash-dotted lines show total, spin-up, and spin-down contributions from 3d-4p transitions in Fe ions respectively. Dash-dot-dotted lines represent contribution from 4s-4p transitions in Fe, and thin solid lines correspond to 4f-5d transitions in rare-earth ions.